NANO LETTERS

2007
Vol. 7, No. 6
1463−1468

Aligned Arrays of Biodegradable Poly(ε-caprolactone) Nanowires and Nanofibers by Template Synthesis

Sarah L. Tao and Tejal A. Desai*

Department or Physiology, University of California, San Francisco, 1700 4th Street, San Francisco, California 94143

Received January 5, 2007; Revised Manuscript Received March 15, 2007

ABSTRACT

We demonstrate that the technically simple, low-cost, and rapid method of template synthesis can be used to create arrays of nanowires and nanofibers from the biocompatible, biodegradable polymer poly(ε-caprolactone) (PCL). PCL substrates introduced into a standard laboratory oven at temperatures as low as 65 °C are able to form nanostructures. Nanostructure morphology can be controlled, and complex patterning can be achieved. Solvent-free and low-temperature fabrications also allow for the encapsulation of therapeutics for sustained release.

Rapid expansion in the fabrication of inorganic nanomaterials, such as oriented carbon nanotubes and nanostructures of semiconductors and metals, has led to great progress in developing materials for miniaturized devices. This interest in ordered, nanostructured materials has translated to applications in biology and medicine with recent findings that cellular responses can be directed by nanotopography. Although inorganic materials are of choice for electronic and mechanical devices, these materials are not necessarily appropriate for applications in biology and medicine. Similar nanostructures fabricated from polymeric biodegradable materials, on the other hand, have great potential for biomedical applications in areas such as tissue engineering and drug delivery. In a physiological environment, cells respond to nanometric topologies such as fibrous and porous materials formed by components of the extracellular matrix. By developing structured nanoscale topographies in synthetic materials, novel scaffolds, microdevices, and implant coatings can be fabricated to mimic the native cellular environment and improve the integration of such artificial constructs.

One standard approach to creating nanoscale topographies is by electrospinning, a process that forms nanofibers through an electrically charged jet of polymer solution. Biodegradable electrospun polymer nanofibers have been extensively studied for applications in the regeneration of tissue due to their high porosity and surface-to-volume ratio.[1−7] Although electrospinning can be used to create nanofibers from a number of different polymers with diameters ranging from less than 3 nm to greater than 1 μm, this process remains dependent on jet stability (due to solvent viscosity, surface tension, and vapor pressure).[8,9] Electrospinning also essentially produces one infinitely long fiber, which is collected in an unordered mesh and is difficult to manipulate into higher order architectures other than uniaxial alignment.[10,11]

Another standard method, which may provide a better means to control the hierarchical structure of the nanostructured surface, is templating. Templating entails synthesizing the desired material within the pores of a membrane.[12] Using a template of aligned and ordered pores produces similarly ordered nanowire arrays perpendicular to the attached substrate. Template synthesis has been previously used to prepare nanotubes and wires from metals[13−15] and semiconductor materials.[16,17] By exploiting methods of electrochemical oxidation, phase separation, extrusion, or wetting in combination with template synthesis, similar structures have also been fabricated in various nondegradable polymers.[12,18−26] However, these materials are not ideal for biomedical applications such as tissue engineering and drug delivery. For such applications, it would be advantageous to create nanoengineered constructs that are able to degrade and be resorbed by the body naturally over time. Nonetheless, template-synthesized nanowires from biodegradable polymers are scarcely reported. Xu et al. described a method of fabricating poly(ε-caprolactone) (PCL) nanofibers by the extrusion of a precursor solution through a template into a solidifying solvent under pressure utilizing custom instrumentation.[27] However, in this work, template synthesis is used to form oriented nanowire and nanofiber arrays from biodegradable polymers without the use of organic solvents, pressure assistance, or custom instrumentation. This fast and inexpensive method of creating biodegradable nanowires and fibers can therefore be used to easily produce nanometric

* Corresponding author. E-mail: tejal.desai@ucsf.edu.

10.1021/nl0700346 CCC: $37.00
Published on Web 05/08/2007

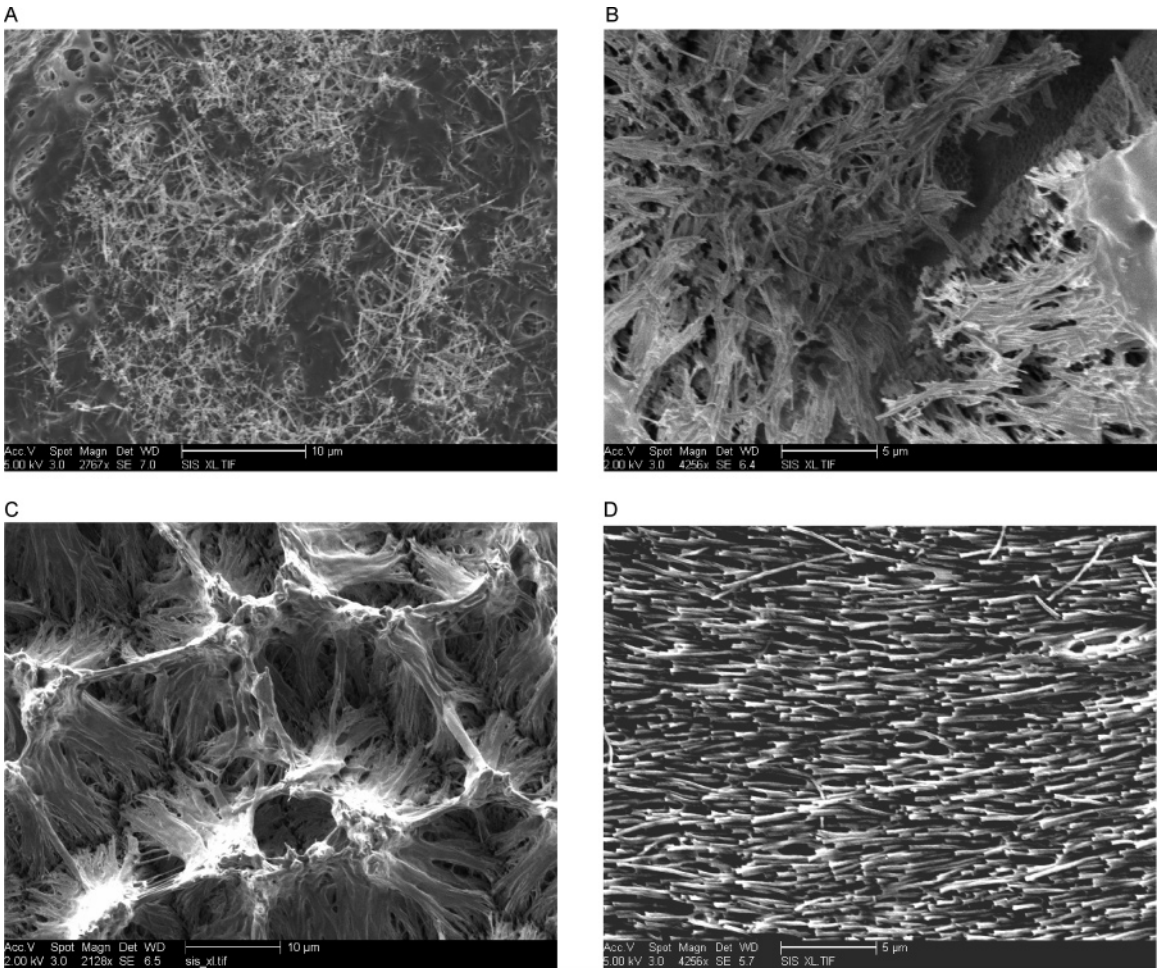

Figure 1. Nanostructures made from biodegradable polymers: (A) 50/50 PLGA, (B) 25/75 DLPLCL, (C) 80/20 DLPLCL, and (D) PCL.

topographies for potential drug delivery and biointegrative applications.

As a template, an aluminum oxide membrane can be used. In general, anodic aluminum oxide films are formed by the electrochemical oxidation of aluminum, as documented in the literature. Depending on the type of anodization process and growth regime used, aluminum oxide membranes can be fabricated to contain nanopores in a wide range of diameters, lengths, and interpore distances.[28−30] In order to facilitate nanowire fabrication, here, commercially available aluminum oxide membrane filters were used instead of custom membranes. The anodized aluminum oxide membranes contained pores 20 nm in diameter, 60 μm in length, and with a porosity of 10^{11} pores/cm^2.

Several biocompatible, biodegradable polymers and composites were utilized for nanostructure formation, including 50/50 poly(DL-lactide-*co*-glycolide) (PLGA) (amorphous, T_g = 45−50 °C), 25/75 poly(DL-lactide-*co*-ε-caprolactone) (25/75 DLPLCL) (amorphous, T_g = 20 °C), 80/20 poly(DL-lactide-*co*-ε-caprolactone) (80/20 DLPLCL) (amorphous, T_g = 20 °C), and PCL (T_m = 58−63 °C, T_g = −65 to −60 °C). Polymer melts were formed at 130 °C while in contact with the nanoporous template. After etching the template in a dilute solution of sodium hydroxide, examination by scanning electron microscopy (SEM) showed that nanostructures could be achieved with all of the polymer melts (Figure 1A−D). However PCL, the only crystalline polymer used, produced the most monodisperse nanowires. Additionally, the PLGA and PLCL polymers have very high melting points, which exclude their use in the encapsulation of drugs, especially proteins, by any melt method. Therefore, PCL was used for all further characterization.

In order to overcome the need for fabricating nanoporous aluminum oxide membranes of varying thickness to produce varying nanowire lengths, nanowire length was instead tuned as a function of melt time and temperature (Figure 2A,B). At a temperature of 130 °C, nanowire lengths of 2.5−27.0 μm could be produced in less than 60 min by varying contact time. At 65 °C, similar structures could be formed; however, increase in nanowire length took place over longer intervals. Nanowires less than 10 μm in length, formed at both 65 and 130 °C, were found to be freestanding (Figure 2C), although the wires shift to pack in loose clusters as the wires are removed from aqueous solution and dried (Figure 2C,E). When greater than 10 μm in length, the nanostructures instead folded over to form long strands of arrayed, flexible nanofibers layered over the substrate base (Figure 2D,F).

No correlation was observed between nanowire diameter and contact time at either temperature. At 130 °C nanowire diameters of 196.1 ± 60.0 nm were observed, and at 65 °C diameters of 168.1 ± 39.1 nm were seen. The difference between the nanowire diameters at the two melting points

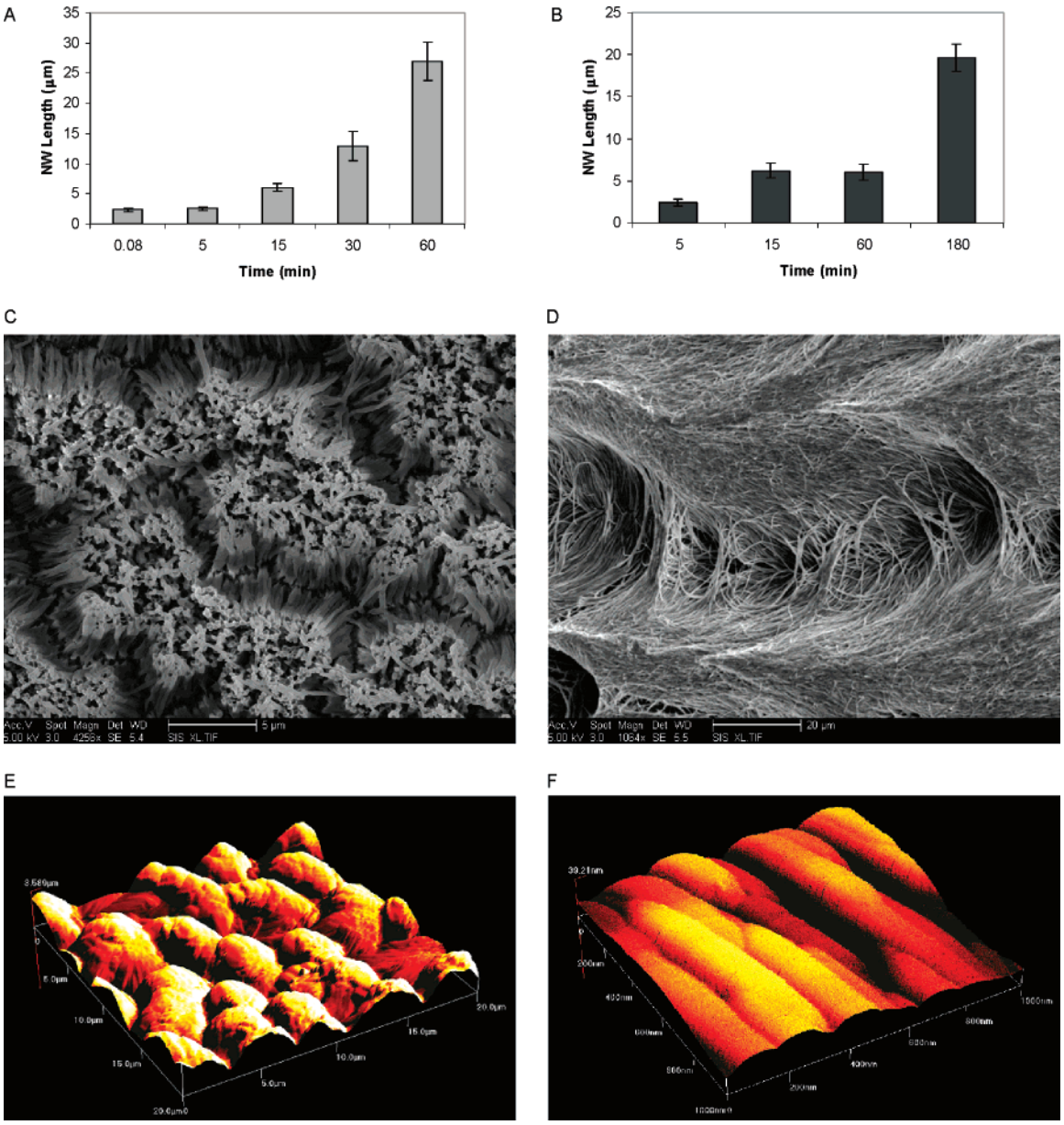

Figure 2. Nanowire morphology as a function of temperature and time. (A) Nanowire length at 130 °C. (B) Nanowire length at 65 °C. (C) SEM image of free-standing array of nanowires 2.5 μm in length. (D) SEM image of an array of flexible nanofibers 27 μm in length. (E) 20 μm intermittent contact AFM 3D image of nanowires 2.5 μm in length. (F) 1 μm intermittent contact AFM image of a nanofiber array.

is statistically significant (one-way ANOVA, $p = 5.2 \times 10^{-5}$) showing that nanowire diameter can be regulated to a certain degree by increasing melt temperature. In both cases, the average nanowire diameter is considerably larger than the template pore size. SEM analysis of the template membrane showed a range of pore diameters with an average diameter of 29.0 ± 9.0 nm, larger than the listed pore diameter, though not significant enough to explain the increase in diameter over theoretical values. A similar increase in nanofiber diameter over pore size has been shown elsewhere.[20,24] It has been suggested that when the diameter of the template pore is smaller than the thickness of the polymer melt traveling along the inside of the pore (typically 10−30 nm), a massive nanowire will form.[24] In this particular situation where the pore diameter is 20 nm, it is possible that the polymer melt cannot be confined within the volume of the pore. Therefore, as the polymer expands during the melt, a larger submicron wire, rather than a nanowire, is created during the template process.

The surface roughness of the PCL nanowires and nanofibers was examined using atomic force microscopy (AFM). In order to capture a representative sample of the topography, 20 μm scan size intermittent contact images were analyzed. As expected, the formation of nanowires on the surface of the PCL increased the roughness of the substrate (Table 1). Both the average roughness (R_a) and the root-mean-square roughness (R_q) increase with nanowire length. The change in wettability due to the surface roughness was investigated using contact angle measurement (Table 1). Contact angles for solvent-cast PCL and PCL treated with heat and exposure to sodium hydroxide etchant were not significantly different. Disks of PCL nanowires, however, were found to have an

Table 1. Surface Roughness Parameters[a]

NW length (μm)	R_a (nm)	R_q (nm)	θ (°)	τ (dynes/cm)
0_a			60.3 ± 4.5	51.7 ± 2.5
0_b	5.9	7.7	66.5 ± 3.8	48.2 ± 2.7
2.5	710.3	822.2	70.0 ± 2.0	45.7 ± 1.5
27	1357	1819	70.7 ± 4.2	45.0 ± 2.6

[a] 0_a = PCL; 0_b = heat, NaOH-treated PCL; R_a = average roughness (20 μm scan size); R_q = root-mean-square roughness (20 μm scan size); θ = water contact angle; τ = wetting tension.

initial contact angle of approximately 16° (nanowires measured less than 20 μm in length) or 32° (nanowires measured greater than 20 μm in length). After dewetting, the disks reached an equilibrium contact angle measurement of approximately 70.3 ± 2.9°, regardless of nanowire length. The heat treatment and exposure to sodium hydroxide did not significantly change the wettability of the PCL; however, the surface roughness of both the free-standing nanowires and flexible nanofibers formed by template synthesis decreased the wettability of the surface (one-way ANOVA, $p = 0.007$, post-hoc Tukey's test). Different models have been proposed to understand the affect of surface roughness on contact angle. The "wetted surface" model assumes that the liquid fills the depressions in the region where it contacts the rough surface,[31] whereas the "composite surface" model dictates that the liquid is lifted up by the roughness features.[32] According to the wetted surface model, the contact angle on arrays of 2.5 and 27 μm nanowires fabricated from the aluminum oxide membrane template will both approach approximately 90.0°. According to the composite surface model, both nanowire arrays should approach a contact angle of 94.4°. Several groups have used experimental results to correlate surface roughness of patterned materials, such as nanowires, with wetted or composite contact angles,[21,33−35] and it has been suggested that, generally, surfaces exhibiting hydrophilic properties ($\theta < 90$°) will follow the wetted surface model for roughness, whereas surfaces exhibiting hydrophobic properties ($\theta > 90$°) will follow the composite surface model, although either can be induced by physical manipulation. The difference between the experimental and theoretical contact angle values here can be attributed to the tight packing of the nanowires as well as the nanowire diameter, as suggested by Martin et al.[21] Here, the compact packing of the nanowires (interpore distance < 20 nm) does not allow either water or air to be trapped between the projections. In the case where distance between wires is negligibly close, the ratio of the rough surface area to the projected area (r) approaches closer to 1. The increase in diameter of the PCL nanowire in comparison to the template pore size causes the contact area with the liquid to increase, and therefore the ratio of the contact area to the rough surface area (f_s) also approaches closer to 1. Similarly, in the case of the nanofiber arrays, the folded-over nanofibers cause a decrease in the projected surface area (as the wires are no longer free-standing), as well as an increase in the liquid contact area. Therefore, the wettability of the nanostructured PCL remains relatively similar to smooth PCL rather than forming superhydrophobic or superhydrophilic surfaces.

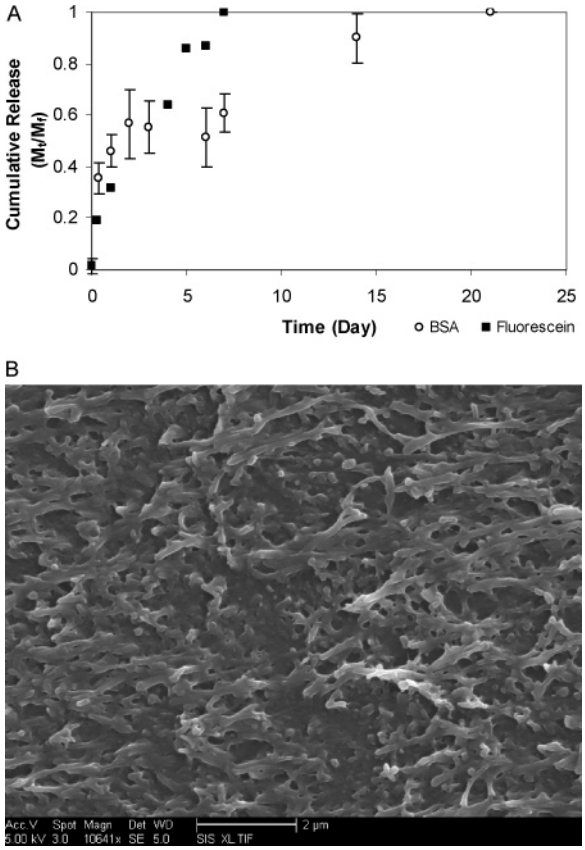

Figure 3. PCL nanowire release and degradation. (A) Cumulative release of fluorescein and BSA from PCL nanowires. (B) SEM image of PCL nanowires after a degradation period of 7 weeks.

As a biocompatible and biodegradable polymer, PCL has been investigated for the controlled delivery of low molecular weight drugs. PCL is known to be highly permeable, though insoluble in water.[36−39] Combined with its high crystallinity and low degradation rate, PCL is well-suited for implantable, long-term drug delivery systems. Potential therapeutic substances such as proteins and peptides may be encapsulated in PCL in the absence of denaturing organic solvents by way of hot-melt encapsulation. Previous studies have shown that melt encapsulation of proteins within PCL produces feasible systems for controlled delivery of stable proteins.[40,41] The method of template synthesis with a PCL polymer melt provides not only a means to fabricate nanowire arrays, but also a potential means to incorporate protein molecules in the nanowires without the use of organic solvents. Here, fluorescein (MW = 389.38 Da, $R_H = 6.5$ Å, $R_G = 9.8$ Å) was used as a small molecule model, and bovine serum albumin (BSA) (MW = 66 kDa, $R_H = 3.7$ nm, $R_G = 2.87$ nm) was used as a model protein for encapsulation and release from PCL nanowires (6 μm in length). Fluorescein was found to release steadily over a period of a week (Figure 3A). A linear regression analysis of the log percent drug released versus log time was performed using the first 60% of the release curve to obtain the diffusional exponent.[42] The diffusional exponent (n) for release of fluorescein from the PCL nanowire substrate ($n = 0.46$, $R^2 = 0.997$) was found to fall in the range $0.43 < n < 0.5$, indicating release controlled by Fickian diffusion.[42] The release profile for

BSA, however, was characterized as a short burst phase during the first 8 h, where approximately 30% of the cumulative protein released was delivered. Sustained release was achieved over a period of 21 days, after which release leveled off and no additional protein was released (Figure 3A). The diffusional exponent for release of BSA from the PCL nanowire substrate ($n = 0.26$, $R^2 = 0.997$) was found to be less than 0.5. It has been previously suggested that drug release from a system with a diffusional exponent less than 0.5 may be due to a combination of diffusion through the matrix and partial diffusion through water-filled pores.[39,42] Therefore, the initial burst in protein release was most likely due to drug desorption at the nanowire surface, where the surrounding fluid is able to begin dissolving exposed protein immediately, whereas the diffusional release phase is attributed to molecule diffusion from near the surface. As the protein at the surface is dissolved, the porosity of the PCL nanowires is increased, allowing fluid to dissolve protein molecules embedded in the nanowire. Protein molecules fully coated and embedded within the nanowire, however, are gradually released due to the hindrance of diffusion of BSA from the inner part of the nanowire. The morphology of the PCL nanowires after degradation in PBS over 7 weeks was observed using SEM. After degradation, the nanowire morphology is less apparent; the nanowires are matted together or degraded completely from the surface (Figure 3B).

The ability to fabricate arrays of nanowires and nanofibers from biodegradable polymers using this fast and inexpensive method of template synthesis holds many advantages over the electrospinning and combination templating methods previously described. First, the method is simple, and there is no need for specialized equipment or setup. Second, the general structure of the nanowires can be controlled by the template design itself. While restricted to a single template design, it is still possible to control nanowire length and, to a degree, nanowire diameter. This allows for the fabrication of aligned arrays of free-standing nanowires or flexible nanofibers rather than an unordered surface. Third, although the presence of densely packed nanowires and nanofibers of PCL decreases the wettability of the surface, the added roughness does not cause drastic changes to form superhydrophobic or superhydrophilic surfaces. Therefore, similar chemical modification processes may be used to alter both smooth and nanowire/fiber PCL surfaces for further control over protein and cell adhesion in biomedical applications. Furthermore, the use of template synthesis allows the nanowires and nanofibers to be loaded with drug molecules without the use of organic solvents, which is especially important in the case of protein and peptide therapeutics. Therefore, the high surface area-to-volume ratio of nanowire/fiber arrays made of PCL would ensure biodegradation and resorption as well as provide a means for delivering controlled doses of bioactive agents locally at the implant site or the site of regeneration.

Furthermore, templating methods for fabricating nanowires and nanofibers from biodegradable polymers may be combined with patterning at the micron level to create biointerfaces with hierarchical nano- and microarchitecture. For example, Figure 4A shows an example of nanofibers patterned in the shape of an 80 μm square atop an array of free-standing nanowires. Other preliminary work has shown that cell morphology may be controlled by subcellular interactions with the nanowire substrates (Figure 4B). The ability to design hierarchical structures on the nano and micro level will allow for even more sophisticated constructs capable of controlling the delivery of therapeutics and cellular responses. The capability to control cell responses at both the nano- and microscale using material properties will be useful not only in the regeneration of hard and soft tissues, but also in determining the biointegration of implantables such as microdevices, stents, orthopedic implants, and biosensors.

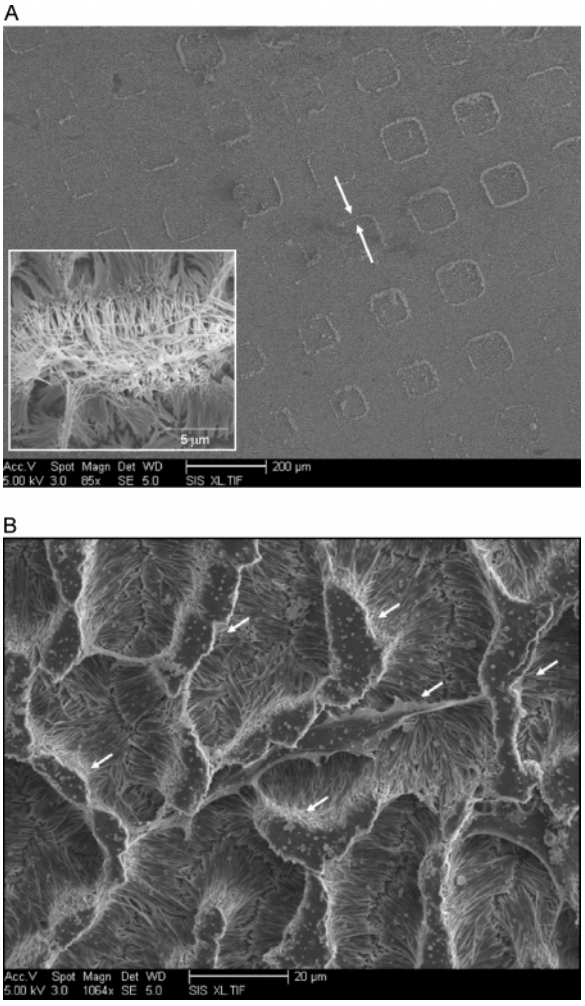

Figure 4. Potential applications of PCL nanowires. (A) SEM image of PCL nanofiber patterns (square outline) atop an array of nanowires. Inset: magnification of the nanofiber/nanowire interface depicted by arrows. (B) SEM image of fibroblast cells interacting on the PCL nanowire surface after 3 days in culture. Arrows point to examples of individual cells.

Acknowledgment. The authors thank the Sandler Family Supporting Foundation and the Knights Templar Eye Foundation. All SEM was performed at the Stanford Nanocharacterization Laboratory through the Stanford CIS grant program.

References

(1) Yoshimoto, H.; Shin, Y. M.; Terai, H.; Vacanti, J. P. *Biomaterials* **2003**, *24*, 2077.
(2) Yang, F.; Murugan, R.; Wang, S.; Ramakrishna, S. *Biomaterials* **2005**, *26*, 2603.
(3) Li, M.; Guo, Y.; Wei, Y.; MacDiarmid, A. G.; Lelkes, P. I. *Biomaterials* **2006**, *27*, 2705.
(4) He, W.; Yong, T.; Teo, W. E.; Ma, Z.; Ramakrishna, S. *Tissue Eng.* **2005**, *11*, 1574.
(5) Venugopal, J.; Ma, L. L.; Yong, T.; Ramakrishna, S. *Cell Biol. Int.* **2005**, *29*, 861.
(6) Chua, K. N.; Lim, W. S.; Zhang, P.; Lu, H.; Wen, J.; Ramakrishna, S.; Leong, K. W.; Mao, H. Q. *Biomaterials* **2005**, *26*, 2537.
(7) Li, W. J.; Tuli, R.; Okafor, C.; Derfoul, A.; Danielson, K. G.; Hall, D. J.; Tuan, R. S. *Biomaterials* **2005**, *26*, 599.
(8) Huang, Z. M.; Zhang, Y. Z.; Kotaki, M.; Ramakrishna, S. *Compos. Sci. Technol.* **2003**, *63*, 2223.
(9) Norman, J.; Desai, T. *Ann. Biomed. Eng.* **2006**, *34*, 89.
(10) Li, D.; Ouyang, G.; McCann, J. T.; Xia, Y. *Nano Lett.* **2005**, *5*, 913.
(11) Li, D.; Wang, Y.; Xia, Y. *Adv. Mater.* **2004**, *16*, 361.
(12) Martin, C. R. *Science* **1994**, *266*, 1961.
(13) Fan, H. J.; Lee, W.; Hauschild, R.; Alexe, M.; Le, Rhun, G.; Scholz, R.; Dadgar, A.; Nielsch, K.; Kalt, H.; Krost, A.; Zacharias, M.; Gosele, U. *Small* **2006**, *2*, 561.
(14) Kline, T. R.; Tian, M. L.; Wang, J. G.; Sen, A.; Chan, M. W. H.; Mallouk, T. E. *Inorg. Chem.* **2006**, *45*, 7555.
(15) Ma, H.; Tao, Z. L.; Gao, F.; Chen, J. *Chin. J. Inorg. Chem.* **2004**, *20*, 1187.
(16) Banerjee, S.; Dan, A.; Chakravorty, D. *J. Mater. Sci.* **2002**, *37*, 4261.
(17) Lombardi, I.; Hochbaum, A. I.; Yang, P. D.; Carraro, C.; Maboudian, R. *Chem. Mater.* **2006**, *18*, 988.
(18) Feng, L.; Li, S.; Li, H.; Zhai, J.; Song, Y.; Jiang, L.; Zhu, D. *Angew. Chem., Int. Ed.* **2002**, *41*, 1221.
(19) Feng, L.; Song, Y.; Zhai, J.; Liu, B.; Xu, J.; Jiang, L.; Zhu, D. *Angew. Chem., Int. Ed.* **2003**, *42*, 800.
(20) Li, H. Y.; Ke, Y. C.; Hu, Y. L. *J. Appl. Polym. Sci.* **2006**, *99*, 1018.
(21) Parthasarathy, R. V.; Martin, C. R. *Chem. Mater.* **1994**, *6*, 1627.
(22) Qiao, J.; Zhang, Z.; Meng, X.; Zhou, S.; Wu, S.; Lee, S. *Nanotechnology* **2005**, *16*, 433.
(23) Rynes, O.; Demoustier-Champagne, S. *J. Electrochem. Soc.* **2005**, *152*, D130.
(24) Steinhart, M.; Wehrspohn, R. B.; Gosele, U.; Wendorff, J. H. *Angew. Chem., Int. Ed.* **2004**, *43*, 1334.
(25) Steinhart, M.; Wendorff, J. H.; Grenier, A.; Wehrspohn, R. B.; Nielsch, K.; Schilling, J.; Choi, J.; Gosele, U. *Science* **2002**, *296*, 1997.
(26) Steinhart, M.; Wendorff, J. H.; Wehrspohn, R. B. *ChemPhysChem* **2003**, *4*, 1171.
(27) Chen, Y.; Zhang, L. N.; Lu, X. Y.; Zhao, N.; Xu, J. *Macromol. Mater. Eng.* **2006**, *291*, 1098.
(28) Lee, W.; Ji, R.; Gosele, U.; Nielsch, K. *Nat. Mater.* **2006**, *5*, 741.
(29) Li, A. P.; Muller, F.; Birner, A.; Nielsch, K.; Gosele, U. *J. Appl. Phys.* **1998**, *84*, 6023.
(30) Masuda, H.; Fukada, K. *Science* **1995**, *268*, 1466.
(31) Wenzel, T. N. *J. Phys. Colloid Chem.* **1949**,1466.
(32) Cassie, A. B. D. *Discuss. Faraday Soc.* **1948**, *3*, 11.
(33) Bico, J.; Tordeux, C.; Quere, D. *Europhys. Lett.* **2001**, *55*, 214.
(34) He, B.; Patankar, N. A.; Lee, J. *Langmuir* **2003**, *19*, 4999.
(35) Patankar, N. A. *Langmuir* **2003**, *19*, 1249.
(36) Bodmeier, R.; Chen, H. *J. Controlled Release* **1989**, *10*, 167.
(37) Livshits, V. S. *Pharm. Chem. J.* **1988**, *22*, 515.
(38) Pitt, C. G.; Jeffcoat, A. R.; Zweidinger, R. A.; Schindler, A. *J. Biomed. Mater. Res.* **1979**, *13*, 497.
(39) Tarvainen, T.; Karjalainen, T.; Malin, M.; Perakorpi, K.; Tuominen, J.; Seppala, J.; Jarvinen, K. *Eur. J. Pharm. Sci.* **2002**, *16*, 323.
(40) Jameela, S. R.; Suma, N.; Jayakrishnan, A. *J. Biomater. Sci., Polym. Ed.* **1997**, *8*, 457.
(41) Lin, W. J.; Yu, C. C. *J. Microencapsulation* **2001**, *18*, 585.
(42) Peppas, N. A. *Pharm. Acta Helv.* **1985**, *60*, 110.

NL0700346